https://doi.org/10.17221/199/2025-RAE

Thin-layer drying kinetics and quality assessment of octopus (*Octopus* sp.) using mixed and open solar dryers

Arina Fatharani[1], Yuwana Yuwana[1], Faulina Maissy[1,2], Firmansyah Firmansyah[1], Hilda Maya Sintia Dewi[3], Ulfah Anis[1], Fitri Yuwita[1]*

[1]*Department of Agricultural Technology, Faculty of Agriculture, University of Bengkulu, Bengkulu, Indonesia*
[2]*Department of Food and Agricultural Product Technology, Andalas University, Padang, Indonesia*
[3]*Department of Agricultural and Biosystems Engineering, Universitas Gadjah Mada, Yogyakarta, Indonesia*

**Corresponding author: arina.fatharani@unib.ac.id*

Citation: Fatharani A., Yuwana Y., Maissy F., Firmansyah F., Dewi H.M.S., Anis U., Yuwita F. (2026): Thin-layer drying kinetics and quality assessment of octopus (*Octopus* sp.) using mixed and open solar dryers. Res. Agr. Eng., 72: 81–94.

Abstract: Octopus (*Octopus* sp.) is highly perishable marine species for which efficient drying is essential to extend shelf life in tropical climates. The anatomical heterogeneity of the octopus complicates consistent drying. This study systematically evaluated the performance of a mixed solar dryer (MSD) and open solar drying (OSD) across distinct anatomical regions (head, mantle, and tentacles), with emphasis on drying kinetics and quality attributes. Five thin-layer models were applied to characterize moisture reduction, and product quality was assessed by measuring browning, protein, fat, and ash content. The MSD achieved a 20% higher temperature and 29% lower humidity, resulting in a 74% increase in drying rate relative to OSD. The Hasibuan and Daud model exhibited the highest predictive accuracy (coefficient of determination (R^2) = 0.9965; root mean square error (RMSE) = 0.0168; sum of squared errors (SSE) = 0.0058). Significant interaction effects between anatomical region and drying method were observed for browning and ash content ($P < 0.05$), whereas protein and fat content were primarily influenced by anatomical characteristics. Overall, the MSD produced products with reduced browning and enhanced nutrient retention. These results support the implementation of MSD technology by small-scale processors to improve both drying efficiency and product quality in octopus preservation.

Keywords: anatomical variation; mixed-mode solar dryer; quality parameters; thin-layer modelling; cephalopod; tropical processing

Octopus (*Octopus* sp.) represents a high-value marine resource, distinguished by its favourable nutritional composition, notably high fibre, low fat, and low carbohydrate content (Xue et al. 2015). The species' pronounced economic significance is evidenced by escalating export volumes, particularly to the European Union, East Asia, and Southeast Asia (Zamuz et al. 2023). At present, postharvest management of octopus is practiced in over 90 countries, with Indonesia among the leading global producers (Sauer et al. 2021; Fall and Asiedu 2024). Within Bengkulu's Kaur Regency, industries are highly dependent on octopus, a commodity inherently susceptible to rapid enzymatic and microbial degradation (Hidrawati et al. 2023; Indrabudi et al. 2025; Pariansyah et al. 2025). The species' elevated moisture content un-

Supported by Lembaga Penelitian dan Pengabdian Kepada Masyarakat (LPPM), University of Bengkulu, through the Pembinaan scheme (contract No. 2064/UN30.15/PP/2023), which was instrumental in facilitating this research.

https://doi.org/10.17221/199/2025-RAE

derscores the necessity for advanced preservation strategies to mitigate postharvest losses (Xue et al. 2020; Hajji et al. 2024).

Although cold storage is widely recognised as an effective preservation strategy, its implementation in remote coastal regions is frequently constrained by elevated energy costs and insufficient infrastructure (Hernández-Urcera et al. 2025). As a result, solar drying has emerged as a cost-effective alternative (Wulfing et al. 2024). Conventional open solar drying (OSD), though prevalent, is susceptible to external environmental variability, contamination, and inconsistent product quality (Nurba et al. 2019; Obot et al. 2022). To overcome these limitations, the mixed solar dryer (MSD) has been developed, incorporating solar collectors to substantially improve drying efficiency (Suherman et al. 2025). MSD technology transfers absorbed solar energy into a controlled chamber, resulting in up to a 55% increase in energy efficiency relative to traditional drying systems (Yassen et al. 2021; Bacha et al. 2025). The integration of UV filters further enhances product safety, preserves quality, and accelerates the drying process by up to 60% (Chemkhi 2022; Mehta et al. 2022; Andharia et al. 2023). Nevertheless, comprehensive engineering evaluations of MSD performance in octopus drying, particularly within tropical coastal settings such as Bengkulu, remain limited.

Alongside hardware advancements, mathematical modelling is essential for clarifying the drying dynamics of agricultural and aquatic commodities (Suherman et al. 2020). Thin-layer kinetic models are widely applied in agricultural engineering due to their methodological simplicity and demonstrated effectiveness in predicting moisture removal (Hii et al. 2023; Schweidtmann et al. 2024). However, the drying of octopus poses a distinct challenge because of significant anatomical heterogeneity. Regions such as the mantle and tentacles differ markedly in muscle architecture, collagen content, and tissue thickness (Jonathan & Egbe 2022; Indrabudi et al. 2025). This inherent structural variability leads to variable drying rates and non-uniform final moisture distributions within a single specimen, a factor that current integrated research has not sufficiently addressed.

This research contributes to the United Nations Sustainable Development Goals (SDGs), specifically SDG 7 (Affordable and Clean Energy) and SDG 9 (Industry, Innovation, and Infrastructure), by facilitating the adoption of energy-efficient technologies in seafood processing (Zhong et al. 2020; Acar et al. 2022). The identified research gap highlights the urgent need for comprehensive studies that systematically compare the efficacy of MSD and OSD for octopus under tropical conditions, develop and validate thin-layer kinetic models tailored to specific anatomical regions, and critically assess the interactive effects of drying method and anatomical structure on key quality metrics, including browning, protein, fat, and ash content. This study provides the first rigorous evaluation of the relationship between anatomical heterogeneity and solar dryer modality (mixed-mode versus open) in influencing both drying kinetics and final product quality in tropical environments. The specific objectives are to: compare the drying efficiency of MSD and OSD for octopus, identify the most suitable thin-layer kinetic models for individual anatomical parts, and clarify the effects of drying strategy and anatomical differentiation on product quality outcomes.

MATERIAL AND METHODS

Material and sample preparation

Fresh octopus (*Octopus* sp.) with an average individual weight of 1.0 ± 0.2 kg were sourced directly from local fishermen in Kaur Regency, Bengkulu Province, Indonesia. Thirty individuals were selected to ensure sufficient biological replication. The octopuses were rinsed with clean water to remove sand and mucus, then drained and weighed. Each specimen was dissected into five anatomical parts (Figure 1): head, mantle, top tentacle, middle tentacle, and bottom tentacle. These segments were further divided to capture natural variation in thickness and structure.

Drying systems and experimental design

The experiment was conducted from November 2023 to January 2024 in Bengkulu, Indonesia, to compare a mixed solar dryer (MSD) and an open solar dryer (OSD). The MSD (Figure 2) comprised a 3 m^2 solar collector connected to an insulated chamber (12 m^3) covered with a 14% UV-filtering sheet. The OSD utilised stainless-steel mesh trays placed on a 1 m high platform, fully exposed to ambient conditions.

A factorial 2 (dryer type: MSD and OSD) × 5 (anatomical part: head, mantle, top tentacle, middle tentacle, and bottom tentacle) experiment

https://doi.org/10.17221/199/2025-RAE

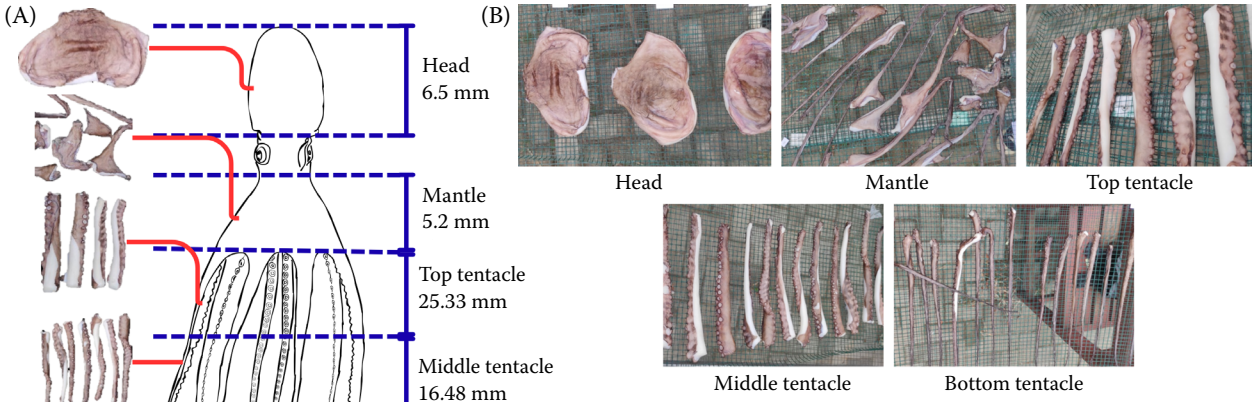

Figure 1. (A) Anatomical regions of the octopus (*Octopus* sp.) (European Union 2022) and (B) detailed segmentation of body parts based on thickness variation

was implemented. From the five homogenised composite samples (one for each anatomical part), representative subsamples were randomly drawn for each experimental run. Drying trials for all ten dryer-part combinations were conducted simultaneously during each run to control for daily weather variation. For each of these combinations, three replicate subsamples (n = 3) were drawn from the corresponding homogenised composite batch. All subsamples were dried concurrently,

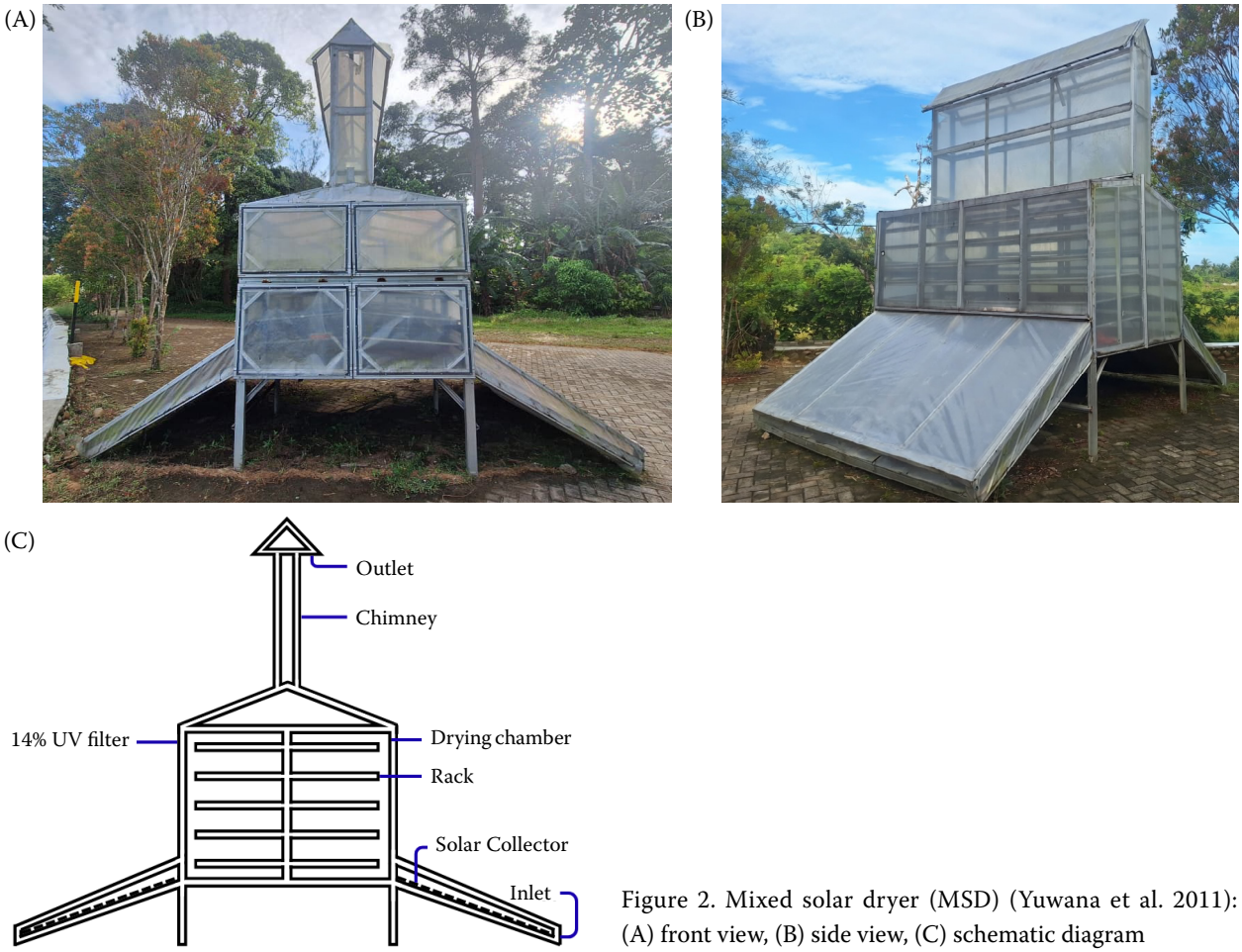

Figure 2. Mixed solar dryer (MSD) (Yuwana et al. 2011): (A) front view, (B) side view, (C) schematic diagram

https://doi.org/10.17221/199/2025-RAE

with the MSD and OSD operated under identical solar conditions to ensure a direct comparison. For each run, fresh subsamples were used. Drying was conducted daily from 08:00 to 16:00. Samples were weighed hourly, and the process was terminated when the moisture content fell below 25% (dry basis) (BSN 2006).

Measurements and data analysis

Drying conditions and mass loss. Air temperature and relative humidity inside the MSD chamber and adjacent to the OSD were recorded hourly using a thermocouple (4 Channels, Type K, HT-9815, Shenzhen Lanqi Technology Co., Ltd., China, accuracy ± 1 °C) and a digital thermos-hygrometer (HTC1, Chongqing New World Trade Co., Ltd, China, accuracy ± 5% RH), respectively. Solar radiation was measured with a solar power meter (SM206, Shenzhen Sanpo Instrument Co.,Ltd ., China, accuracy ± 10 $W \cdot m^{-2}$). Sample mass was recorded hourly using a digital scale (I-2000, Shanghai Dahua Scale Factory, China, accuracy ± 0.1 g). Surface colour (CIE L^*, a^*, b^*) was evaluated with a colourimeter (LS171 D/8, Shenzhen Linshang Technology Co., Ltd., China, accuracy > 90%). The quality of dried octopus, including browning, protein, fat, and ash content, was assessed after drying.

Calculation of drying parameters. The initial moisture content was determined using the thermogravimetric method, as described by Equations (1) and (2) (Deeto et al. 2018):

$$M_{(\mathrm{wb})}(\%) = \frac{M_0 - M_i}{M_0} \times 100\% \quad (1)$$

$$MC_{(\mathrm{db})} = \frac{M_0 - M_i}{M_i} \times 100 \quad (2)$$

where: $M_{(\mathrm{wb})}$ – the moisture content on a wet basis (%); $M_{(\mathrm{db})}$ – the moisture content on a dry basis expressed as an absolute value ($kg \cdot kg^{-1}$); M_0 – the initial mass before drying (g); M_i – the bone-dry sample mass after drying (g).

The drying rate was calculated based on moisture content using Equation (3) (Jonathan & Egbe 2022):

$$DR = \frac{\Delta MC}{\Delta t} \quad (3)$$

where: DR – drying rate ($kg \cdot kg^{-1} \cdot h^{-1}$); ΔMC – the change in moisture content on a dry basis ($kg \cdot kg^{-1} \cdot h^{-1}$); Δt – the time interval (h) during the drying period.

Moisture content (MC) was also expressed as moisture ratio (MR) using Equation (4) (Delfiya et al. 2020):

$$MR = \frac{MC - MC_\mathrm{e}}{MC_0 - MC_\mathrm{e}} \approx \frac{M_t}{\mathrm{M}_0} \quad (4)$$

where: M – the dry-based moisture content ($kg \cdot kg^{-1}$) at time t; M_0 – the initial dry-based moisture content ($kg \cdot kg^{-1}$); and MC_e is the equilibrium dry-based moisture content ($kg \cdot kg^{-1}$) which was neglected in this study due to its relatively small value under experimental conditions.

Mathematical modelling of drying kinetics

Experimental MR data for each treatment were fitted to five thin-layer drying models (Table 1). Model parameters were estimated by non-linear regression, maximising the coefficient of determination (R^2) and minimising the root mean square error (RMSE) and sum of squared errors (SSE). All models were evaluated using Python (version 3.13.2).

Model goodness-of-fit was evaluated using Equations (5) to (7). The model with the highest R^2 and the lowest RMSE and SSE was selected as optimal (Biswas et al. 2022).

$$R^2 = 1 - \frac{\sum_1^n \left(MR_{(\exp,i)} - MR_{(\mathrm{pred},i)}\right)^2}{\sum_i^n \left(MR_{(\exp,i)} - \overline{MR}\right)^2} \quad (5)$$

$$\mathrm{RMSE} = \sqrt{\frac{\sum_i^n \left(MR_{(\exp,i)} - MR_{(\mathrm{pred},i)}\right)^2}{N}} \quad (6)$$

$$\mathrm{SSE} = \frac{1}{N}\sum_i^n \left(MR_{(\exp,i)} - MR_{(\mathrm{pred},i)}\right)^2 \quad (7)$$

Quality assessment

The quality of dried octopus was assessed by measuring browning and proximate composi-

Table 1. Thin-layer kinetics modelling (Inyang et al. 2018)

Model name	Model
Logarithmic	$MR = ae^{-kt} + c$
Midilli et al.	$MR = ae^{-ktn} + bt$
Balbay and Sahin	$MR = (1 - a)e^{-ktn} + b$
Hasibuan and Daud	$MR = 1 - at^n e^{-ktn}$
Demir et al.	$MR = ae^{(-kt)n} + b$

MR – moisture ratio

https://doi.org/10.17221/199/2025-RAE

tion, including protein, fat, and ash content. The browning index (B^*) was determined from L^*, a^*, and b^* values using Equations (8) and (9) (Hu et al. 2024):

$$x = \frac{a^* + 1.75 \times L^*}{5.645 \times L^* + a^* - 3.012 \times b^*} \quad (8)$$

$$B^* = \frac{100 \times (x - 0.31)}{0.172} \quad (9)$$

where: L^*, a^*, and b^* – lightness, redness, and yellowness, respectively, as measured by a colourimeter.

Proximate composition was determined as follows: protein content by the Kjeldahl method (Sudarmadji et al. 1997), fat content by Soxhlet extraction with n-hexane (Talumepa et al. 2016), and ash content by the dry ashing method at 550 °C (BSN 2006). These parameters were analysed using Equations (10) to (12).

$$\text{Protein}(\%) = \frac{V \times N \times 14 \times 6.25 \times P}{M} 100\% \quad (10)$$

$$\text{Fat}(\%) = \frac{W_3 - W_1}{W_2} 100\% \quad (11)$$

$$\text{Ash}(\%) = \frac{B - A}{M} 100\% \quad (12)$$

where: V – the sample titration volume (mL); N – the normality of the H_2SO_4 solution; P – the dilution factor; W_1 – the weight of the empty fat flask (g); W_2 – the sample weight (g), W_3 – the weight of the fat flask containing extracted fat (g); A – the weight of the empty porcelain ash cup (g); B – the weight of the porcelain ash cup containing sample ash (g).

All analyses were performed in triplicate on dried, homogenised powder, and results are expressed on a dry weight basis.

Statistical analysis

The effects of drying method, anatomical part, and their interaction on all quality parameters were analysed using a 2 × 5 factorial of analysis of variance (ANOVA). When a significant effect was detected ($P < 0.05$), mean separation was performed using Duncan's multiple range test (DMRT). Data are presented as mean ± standard deviation.

RESULTS AND DISCUSSION

Drying environmental conditions. Figure 3 presents the environmental parameters influencing the drying process, specifically temperature, relative humidity (RH), and solar irradiance. The MSD, equipped with a 14% UV-filtering cover, significantly reduced incident solar radiation within the drying chamber (average 447.5 W·m^{-2}), compared

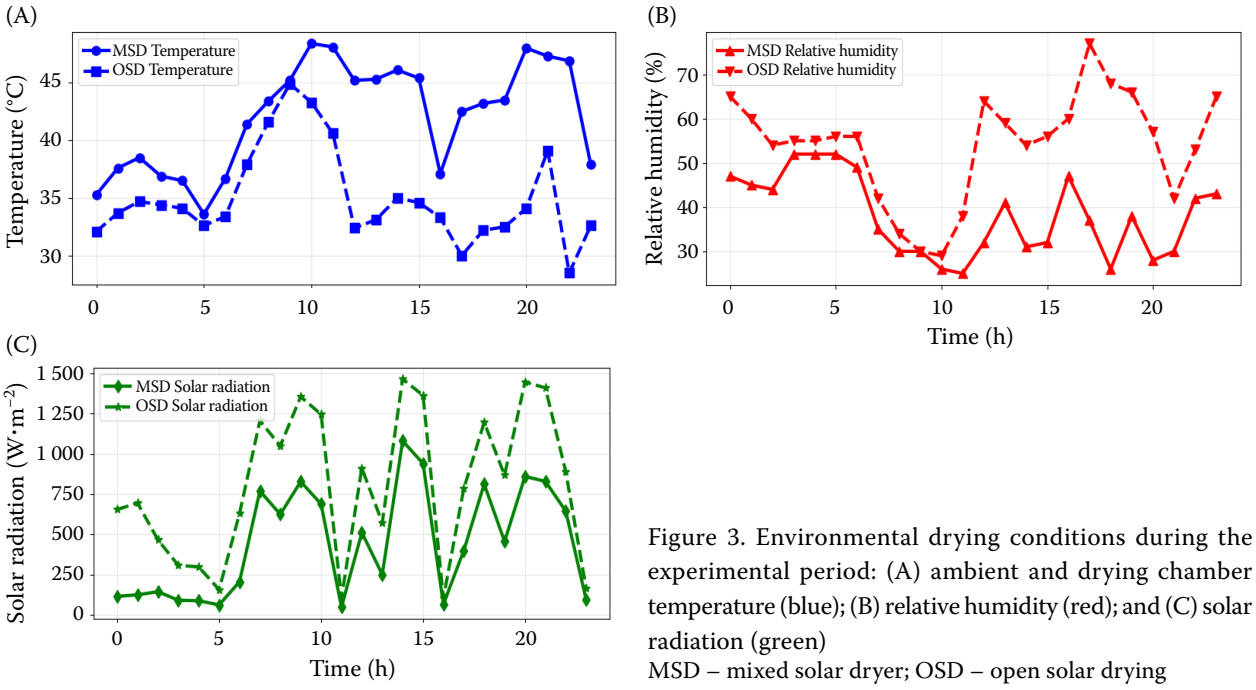

Figure 3. Environmental drying conditions during the experimental period: (A) ambient and drying chamber temperature (blue); (B) relative humidity (red); and (C) solar radiation (green)
MSD – mixed solar dryer; OSD – open solar drying

https://doi.org/10.17221/199/2025-RAE

to the OSD system, which remained fully exposed to ambient irradiance (average 806.5 W·m^{-2}).

Peak ambient solar radiation of approximately 1 400 W·m^{-2} is consistent with cloud-edge enhancement and localised reflective effects documented in diverse global settings. These irradiance surges primarily arise from partially cloudy conditions and dynamic cloud characteristics, including cloud type, spatial distribution, and movement relative to the solar path (Inman et al. 2016; Vamvakas et al. 2020). Inman et al. (2016) reported cloud-enhanced global horizontal irradiance exceeding 1 000 W·m^{-2} in California and Hawaii, attributing these increases to forward scattering by cumulus clouds near the solar disk. Such enhancements occur frequently and significantly influence coastal surface radiation budgets. Similarly, Vamvakas et al. (2020) observed transient cloud-induced enhancements in Patras, Greece, with magnitude dependent on cloud type, position, and movement relative to the sun. Recent research has elucidated the underlying mechanisms. Zuo et al. (2024) introduced a three-dimensional cloud index (CT) based on all-sky image luminance, demonstrating that enhancement primarily occurs when clouds are within three solar radii of the sun. In Colorado, irradiance values reached 1244 W·m^{-2}, with cloud modification factors (CMF) exceeding 1.4 under partially cloudy conditions. Hu et al. (2025) identified solar elevation angle as the primary determinant, with cooling effects prevailing at angles above 63°. Extreme irradiance values surpassing the solar constant have been documented in tropical regions. For instance, De Andrade and Tiba (2016) recorded up to 1650 W·m^{-2} in northeastern Brazil (9°S), approximately 350 W·m^{-2} above extraterrestrial irradiance, on one-third of days per month for up to 34 minutes. Piacentini et al. (2011) measured 1 477 W·m^{-2} at sea level in Recife, Brazil, exceeding the corrected solar constant by 7.9% on 3.4% of days. The tropical coastal environment of Bengkulu (≈ 4°S) is conducive to such events due to consistently high solar elevation, frequent cumulus cloud development typical of maritime tropics, and localised reflection from the Indian Ocean. Budiyanto et al. (2020) established baseline turbidity factors (A = 0.88, B = 0.26) for clear-sky conditions in Indonesia. Therefore, the observed peak of approximately 1 400 W·m^{-2} is consistent with established scientific understanding of cloud-radiation interactions and represents a physically credible measurement under partially cloudy tropical conditions.

Although the MSD received lower direct irradiance, its integrated solar collector effectively captured and converted thermal energy, resulting in a consistently higher average drying air temperature (42.1 °C), approximately 20% greater than the OSD average (35.0 °C). These findings align with those of Kuhe et al. (2019), highlighting the effectiveness of MSD configurations in optimising drying microclimates. The superior drying performance of the MSD can be attributed to its enclosed design and integrated solar air heater, which collectively increase the drying air temperature and enhance the air's moisture-holding capacity. This configuration resulted in an average relative humidity (RH) of 38.1% within the MSD chamber, compared to 54.0% ambient RH observed around the fully exposed OSD trays. The 29% reduction in RH, driven by the efficient thermal energy retention and restricted moisture exchange with the external environment, proved critical in accelerating drying kinetics and generating a substantially greater thermodynamic driving force for moisture removal (Bacha et al. 2025; Suherman et al. 2025). In contrast, the OSD system, subject to ambient variability, demonstrated reduced drying efficiency consistent with the documented limitations of traditional open-air drying methodologies (Duong et al. 2021; Nurba et al. 2019).

Drying kinetics: Assessment of moisture profiles and drying rates. The drying profiles for all octopus anatomical regions exhibited a characteristic exponential reduction in absolute moisture content (kg·kg^{-1}) (Figure 4A), with the drying process markedly more efficient in the MSD relative to the OSD system. Transformation of these data into moisture ratio (*MR*, Figure 4B) facilitated standardised inter-anatomical comparisons and established a robust basis for subsequent thin-layer kinetic modelling.

Analysis of the drying rate (*DR*) revealed that the drying process predominantly transpired within a protracted falling-rate period (Figure 5A), a characteristic commonly observed in biological matrices wherein internal moisture diffusion governs the overall drying kinetics. The absence of a discernible initial constant-rate phase indicates rapid removal of surface-bound moisture. Notably, the average *DR* achieved in the MSD was 74% greater

https://doi.org/10.17221/199/2025-RAE

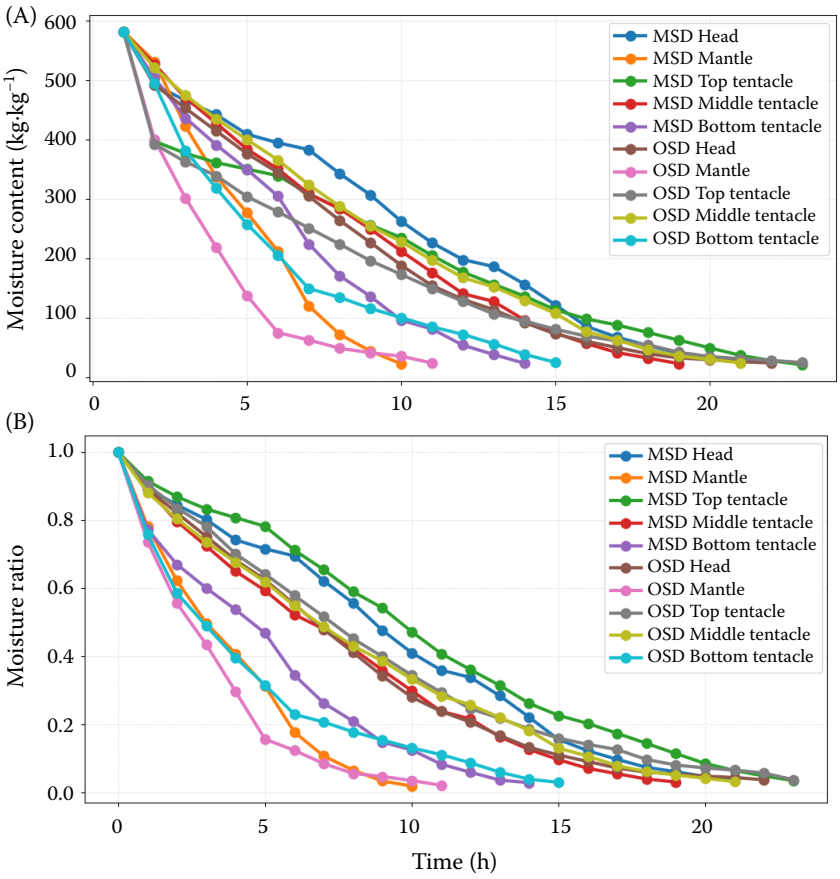

Figure 4. Drying curves of octopus parts: (A) moisture content (dry basis) and (B) moisture ratio
MSD – mixed solar dryer; OSD – open solar drying

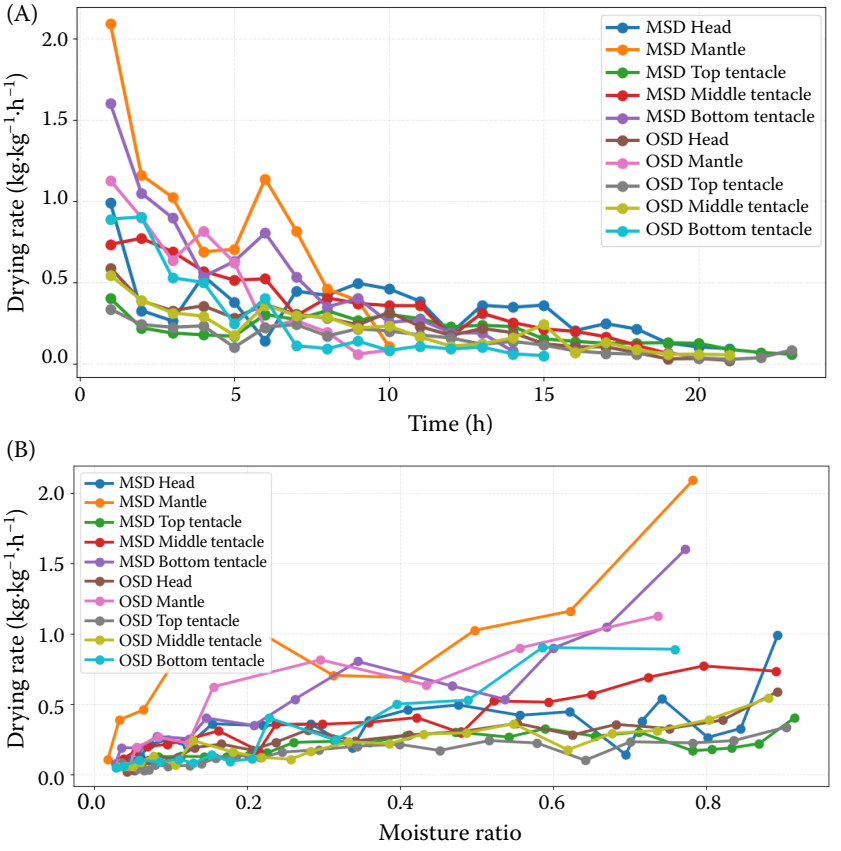

Figure 5. Drying rate analysis: (A) drying rate vs. time, (B) drying rate vs. moisture ratio
MSD – mixed solar dryer; OSD – open solar drying

https://doi.org/10.17221/199/2025-RAE

(0.47 kg·kg^{-1}·h^{-1}) than in the OSD (0.27 kg·kg^{-1}·h^{-1}), thereby explaining the markedly steeper moisture loss profiles depicted in Figure 4. This pronounced enhancement is congruent with performance improvements previously reported for MSD technologies (Ekka and Palanisamy 2021).

Analysis of the *DR* as a function of moisture content *MC* (Figure 5B) indicates that the trendlines for the MSD consistently surpass those of the OSD system throughout the entire moisture range. This finding highlights the MSD's ability to sustain a greater driving force for evaporation during all phases of the drying process. Such performance is characteristic of advanced controlled thermal drying systems, where higher temperatures and lower relative humidity promote a steeper vapour pressure gradient between the material and the drying air (Vengsungnle et al. 2020).

Pronounced morphological heterogeneity in octopus specimens results in substantial variability in drying kinetics, regardless of the drying system used. The mantle and bottom tentacles display drying rates nearly twice those of the thicker head and middle tentacles, as indicated by the steeper gradients in Figures 4 and 5. Drying rates stagnate in more robust anatomical regions at approximately 42 °C, indicating a thermal threshold that solar-based drying systems cannot overcome during periods of reduced irradiance. This heterogeneity is primarily determined by tissue thickness, which controls the internal moisture diffusion path length. Shorter path lengths and higher surface-area-to-volume ratios significantly accelerate water removal. These results support established principles in agricultural engineering, where material geometry is a key factor influencing drying rates (Lakshmi et al. 2021; Ghanem et al. 2025), and underscore the need for anatomically tailored drying protocols in complex cephalopod matrices (Hajji et al. 2024; Indrabudi et al. 2025).

Thin-layer drying kinetics and model selection. Experimental *MR* data obtained from both drying modalities and all anatomical regions were systematically fitted to five established thin-layer models (Logarithmic, Midilli et al., Balbay and Sahin, Hasibuan and Daud, and Demir et al.). Goodness-of-fit statistics (R^2, RMSE, and SSE) for all models across treatments are summarised in Table 2. The Hasibuan and Daud model demonstrated the highest predictive accuracy, achieving the highest average R^2 (0.9965) and the lowest error estimates (RMSE = 0.0168; SSE = 0.0058) among all models. The superior performance is attributed to the model's mathematical flexibility, which allows for accurate characterisation of the complex drying dynamics of octopus tissue, particularly the rapid initial moisture loss and the extended tailing period observed in the drying profiles (Figures 4B, 6).

While conventional exponential models may adequately represent drying kinetics in homogeneous biological matrices, the complex and heterogeneous muscle architecture of octopus tissue requires the greater flexibility provided by the Hasibuan and Daud model parameters. For instance, although the Page model has been widely recognised as optimal for fish skin (Fikry et al. 2023), current findings suggest that morphologically intricate cephalopod tissues necessitate more adaptable modelling approaches. This conclusion aligns with recent research on dense aquatic proteins, such as African catfish (*Clarias gariepinus*) (Agyei et al. 2025) and Asian Seabass (*Lates calcarifer*) fish skin (Fikry et al. 2023), where multi-parameter models have been shown to more accurately characterise distinct drying behaviours. The close agreement between empirical data and the Hasibuan and Daud model, as shown in Figure 6, highlights the model's ability to reliably predict moisture ratio dynamics during octopus drying.

Quality attributes of dried octopus. The ultimate quality of dried octopus was significantly influenced by both the drying method and the inherent anatomical heterogeneity. Table 3 presents the results of a comprehensive factorial ANOVA, detailing the main and interactive effects of dryer type and anatomical region. Table 4 summarises the associated physical and chemical quality attributes and their statistical significance levels.

Analysis of variance (ANOVA, Table 3) indicated that the browning index was significantly affected by dryer type, anatomical region, and their interaction ($P < 0.01$). Both drying modality and anatomical specificity had substantial impacts on the final quality attributes of dried octopus, with the MSD consistently producing superior results. The browning index (B^*) was significantly lower in MSD-treated samples compared to those processed by OSD ($P < 0.05$). For example, the mantle section dried with the MSD had a B^* value of 13.00 ± 0.32, while the top tentacle dried using OSD reached 40.60 ± 0.26 (Table 4). In the head

https://doi.org/10.17221/199/2025-RAE

Table 2. Equation and goodness-of-fit statistics for thin-layer drying models of octopus parts

Model name	Dryer	Body part	Equation	R^2	RMSE	SSE
Logarithmic	MSD	head	$MR = 2.02e^{-0.03t} - 1.02$	0.991	0.030	0.020
	MSD	mantle	$MR = 1.20e^{-0.18t} - 0.21$	0.996	0.020	0.004
	MSD	top tentacle	$MR = 1.86e^{-0.03t} - 0.84$	0.992	0.028	0.019
	MSD	middle tentacle	$MR = 1.29e^{-0.08t} - 0.30$	0.998	0.014	0.004
	MSD	bottom tentacle	$MR = 1.14e^{-0.13t} - 0.17$	0.992	0.027	0.011
	OSD	head	$MR = 1.17e^{-0.10t} - 0.15$	0.993	0.025	0.014
	OSD	mantle	$MR = 1.05e^{-0.29t} - 0.05$	0.995	0.021	0.005
	OSD	top tentacle	$MR = 1.17e^{-0.09t} - 0.15$	0.997	0.018	0.008
	OSD	middle tentacle	$MR = 1.24e^{-0.08t} - 0.25$	0.998	0.012	0.003
	OSD	bottom tentacle	$MR = 0.95e^{-0.24t} + 0.03$	0.996	0.016	0.004
Midilli et al.	MSD	head	$MR = 0.94e^{-0.02t^{1.56}} - 0.004t$	0.994	0.025	0.013
	MSD	mantle	$MR = 0.99e^{-0.20t^{1.02}} - 0.012t$	0.996	0.021	0.005
	MSD	top tentacle	$MR = 0.95e^{-0.02t^{1.63}} - 0.002t$	0.997	0.016	0.006
	MSD	middle tentacle	$MR = 0.99e^{-0.08t^{1.08}} - 0.007t$	0.998	0.014	0.004
	MSD	bottom tentacle	$MR = 0.98e^{-0.17t^{0.92}} - 0.011t$	0.992	0.027	0.011
	OSD	head	$MR = 0.96e^{-0.05t^{1.38}} - 0.00003t$	0.998	0.014	0.005
	OSD	mantle	$MR = 0.99e^{-0.26t^{1.13}} - 0.0004t$	0.996	0.019	0.004
	OSD	top tentacle	$MR = 0.98e^{-0.05t^{1.28}} - 0.0004t$	0.999	0.010	0.002
	OSD	middle tentacle	$MR = 0.98e^{-0.08t^{1.08}} - 0.0054t$	0.998	0.013	0.003
	OSD	bottom tentacle	$MR = 1.00e^{-0.29t^{0.86}} - 0.0012t$	0.998	0.011	0.002
Balbay and Sahin	MSD	head	$MR = (1 + 0.07)e^{-0.02t^{1.50}} - 0.13$	0.994	0.025	0.014
	MSD	mantle	$MR = (1 + 0.20)e^{-0.18t^{1.00}} - 0.21$	0.996	0.020	0.004
	MSD	top tentacle	$MR = (1 + 0.002)e^{-0.02t^{1.61}} - 0.05$	0.997	0.016	0.007
	MSD	middle tentacle	$MR = (1 + 0.23)e^{-0.07t^{1.05}} - 0.24$	0.998	0.013	0.004
	MSD	bottom tentacle	$MR = (1 + 0.29)e^{-0.14t^{0.89}} - 0.30$	0.992	0.026	0.010
	OSD	head	$MR = (1 - 0.03)e^{-0.05t^{1.38}} - 0.003$	0.998	0.014	0.005
	OSD	mantle	$MR = (1 - 10^{-4})e^{-0.26t^{1.12}} - 0.01$	0.996	0.019	0.004
	OSD	top tentacle	$MR = (1 - 0.01)e^{-0.05t^{1.27}} - 0.01$	0.999	0.010	0.002
	OSD	middle tentacle	$MR = (1 + 0.18)e^{-0.07t^{1.05}} - 0.20$	0.998	0.012	0.003
	OSD	bottom tentacle	$MR = (1 + 0.02)e^{-0.28t^{0.85}} - 0.02$	0.998	0.012	0.002
Hasibuan and Daud	MSD	head	$MR = 1 - 0.05t^{1.16}e^{-0.02t^{1.16}}$	0.992	0.028	0.017
	MSD	mantle	$MR = 1 - 0.22t^{0.96}e^{-0.08t^{0.96}}$	0.996	0.019	0.004
	MSD	top tentacle	$MR = 1 - 0.03t^{1.30}e^{-0.01t^{1.30}}$	0.996	0.020	0.010
	MSD	middle tentacle	$MR = 1 - 0.10t^{0.98}e^{-0.03t^{0.98}}$	0.998	0.013	0.003
	MSD	bottom tentacle	$MR = 1 - 0.19t^{0.84}e^{-0.06t^{0.84}}$	0.992	0.026	0.010
	OSD	head	$MR = 1 - 0.07t^{1.16}e^{-0.03t^{1.16}}$	0.998	0.013	0.004
	OSD	mantle	$MR = 1 - 0.27t^{1.00}e^{-0.10t^{1.00}}$	0.997	0.016	0.003
	OSD	top tentacle	$MR = 1 - 0.07t^{1.11}e^{-0.03t^{1.11}}$	0.999	0.009	0.002
	OSD	middle tentacle	$MR = 1 - 0.10t^{0.97}e^{-0.03t^{0.97}}$	0.999	0.011	0.003
	OSD	bottom tentacle	$MR = 1 - 0.29t^{0.77}e^{-0.11t^{0.77}}$	0.998	0.013	0.003
Demir et al.	MSD	head	$MR = 2.02e^{(-0.06\ t)^{0.58}} - 1.02$	0.991	0.030	0.020
	MSD	mantle	$MR = 1.20e^{(-0.13\ t)^{1.36}} - 0.21$	0.996	0.020	0.004
	MSD	top tentacle	$MR = 1.86e^{(-0.06\ t)^{0.61}} - 0.84$	0.992	0.028	0.019
	MSD	middle tentacle	$MR = 1.29e^{(-0.09\ t)^{0.88}} - 0.30$	0.998	0.014	0.004

https://doi.org/10.17221/199/2025-RAE

Table 2 to be continued

Model name	Dryer	Body part	Equation	R^2	RMSE	SSE
Demir et al.	MSD	bottom tentacle	$MR = 1.14e^{(-0.14\,t)^{0.97}} - 0.17$	0.992	0.027	0.011
	OSD	head	$MR = 1.17e^{(-0.09\,t)^{1.03}} - 0.15$	0.993	0.025	0.014
	OSD	mantle	$MR = 1.05e^{(-0.21\,t)^{1.36}} - 0.05$	0.995	0.021	0.005
	OSD	top tentacle	$MR = 1.17e^{(-0.09\,t)^{1.92}} - 0.15$	0.997	0.018	0.008
	OSD	middle tentacle	$MR = 1.24e^{(-0.07\,t)^{1.03}} - 0.25$	0.998	0.012	0.003
	OSD	bottom tentacle	$MR = 0.95e^{(-0.17\,t)^{1.41}} + 0.03$	0.996	0.016	0.004

MSD – mixed solar dryer; OSD – open solar drying; *MR* – moisture ratio; R^2 – coefficient of determination; RMSE – root mean square error; SSE – sum of squared errors

region, the browning value for OSD (41.15) was 2.05 times higher than that observed in the MSD (20.07). This difference is attributed to the UV-filtering cover in the MSD, which reduced Maillard reactions and non-enzymatic browning by protecting the product from direct, high-energy radiation (Fatharani et al. 2025). The significant interaction between drying method and anatomical part highlights that colour degradation is influenced not only by the drying technique but also by the inherent thickness and structural characteristics of octopus tissue, which affect the penetration of heat and radiation through muscle fibres.

Analysis of variance (ANOVA) revealed that both dryer type ($P = 0.001$) and anatomical region ($P < 0.001$) had significant main effects on protein content, whereas their interaction was not significant ($P = 0.635$) (Table 3). The lack of a significant interaction suggests that the influence of dryer type on protein retention remained consistent across all anatomical regions. While samples processed with the MSD showed slightly higher nominal protein values, post-hoc comparisons (Table 4) did not identify statistically significant differences among specific dryer-anatomical region combinations, as indicated by shared superscript notation.

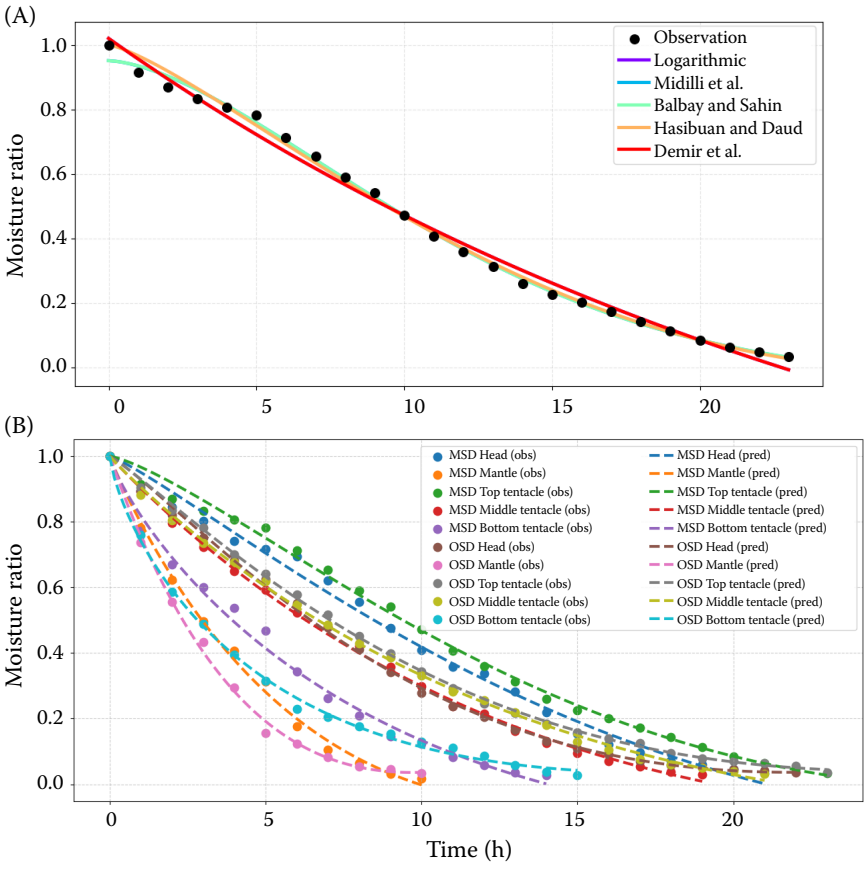

Figure 6. (A) Comparison of all models and (B) detailed fitting of the Hasibuan and Daud model
MSD – mixed solar dryer; OSD – open solar drying

https://doi.org/10.17221/199/2025-RAE

Table 3. Summary of factorial analysis of variance (ANOVA) for the quality parameters of dried octopus

Quality parameter	Source of variation	SS	*df*	MS	*F*-value	*P*-value
Browning	dryer type (D)	380.849	1	380.849	23.431	< 0.001*
	body part (P)	1 841.159	4	460.290	28.319	< 0.001*
	interaction (D × P)	352.267	4	88.067	5.418	0.004*
	error	325.076	20	16.254		
Protein content	D	43.140	1	43.140	13.673	0.001*
	P	554.539	4	138.635	43.939	< 0.001*
	D × P	8.170	4	2.043	0.647	0.635^{ns}
	error	63.103	20	3.155		
Fat content	D	0.974	1	0.974	2.146	0.158^{ns}
	P	76.115	4	19.029	41.944	< 0.001*
	D × P	3.789	4	0.947	2.088	0.120^{ns}
	error	9.073	20	0.454		
Ash content	D	0.035	1	0.035	9.018	0.007*
	P	12.057	4	3.014	779.745	< 0.001*
	D × P	0.475	4	0.119	30.715	< 0.001*
	error	0.077	20	0.004		

df – degrees of freedom; SS – sum of squares; MS – mean square; *significant ($P < 0.05$); ^{ns}non-significant

This result is explained by the non-significant interaction, which means the beneficial effect of the MSD observed in ANOVA was uniformly distributed across anatomical parts and thus not detectable in pairwise comparisons. However, the significant main effect of dryer type indicates that the more controlled thermal environment of the MSD (35.0–42.1 °C) provided modestly improved preservation of total nitrogen compared to the variable conditions of the OSD system. It should be noted that the Kjeldahl method quantifies total nitrogen, which may not fully reflect protein digestibility or functional integrity. Further studies using advanced protein analysis are recommended to complement these findings.

Fat content was primarily determined by anatomical region ($P < 0.001$), while the drying method did not exert a statistically significant main effect ($P = 0.158$). However, pairwise comparisons (Table 4) revealed that samples processed with

Table 4. Physical and chemical characteristics of dried octopus

Dryer	Body part	Quality of dried octopus			
		browning	protein	fat	ash
MSD	head	20.07 ± 0.33^{e}	48.02 ± 2.30^{a}	14.43 ± 0.83^{a}	5.97 ± 0.03^{de}
	mantle	13.00 ± 0.32^{a}	53.54 ± 2.24^{a}	18.58 ± 0.84^{a}	4.33 ± 0.05^{a}
	top tentacle	25.31 ± 0.41^{g}	50.53 ± 1.53^{a}	16.31 ± 0.59^{a}	5.68 ± 0.02^{bc}
	middle tentacle	22.72 ± 0.24^{f}	45.83 ± 0.77^{a}	18.15 ± 0.65^{a}	5.39 ± 0.05^{cd}
	bottom tentacle	16.07 ± 0.48^{c}	56.74 ± 0.74^{a}	17.13 ± 0.09^{a}	4.46 ± 0.01^{a}
OSD	head	41.15 ± 0.33^{h}	44.63 ± 2.19^{a}	13.03 ± 0.50^{a}	6.03 ± 0.04^{f}
	mantle	14.04 ± 0.42^{b}	52.50 ± 1.31^{a}	17.61 ± 0.64^{a}	4.78 ± 0.10^{ab}
	top tentacle	40.60 ± 0.26^{h}	46.48 ± 1.42^{a}	15.95 ± 0.24^{a}	5.93 ± 0.13^{de}
	middle tentacle	23.03 ± 0.20^{f}	42.93 ± 1.37^{a}	17.33 ± 0.67^{a}	5.16 ± 0.02^{ef}
	bottom tentacle	19.45 ± 0.30^{d}	55.13 ± 1.75^{a}	18.13 ± 0.13^{a}	4.33 ± 0.13^{a}

MSD – mixed solar dryer; OSD – open solar drying; in the same column, different letters indicate significant differences at $P < 0.05$ Duncan's multiple range test

https://doi.org/10.17221/199/2025-RAE

the MSD generally retained more fat, particularly in the mantle (up to 18.58 ± 0.84%). This finding indicates that the enclosed, UV-filtered environment of the MSD chamber reduced lipid oxidation. In contrast, the OSD system subjected samples to prolonged elevated temperatures and direct ultraviolet radiation, both recognised as drivers of oxidative rancidity in marine products (Shen et al. 2024). The pronounced susceptibility of lipid constituents to degradation under thermally unstable conditions highlights the need for consistent and elevated thermal inputs to better control oxidative mechanisms during the drying of high-fat marine matrices.

All samples met established ash content quality standards (< 7%) (BSN 2017). Analysis of variance revealed a highly significant interaction between dryer type and anatomical region ($P < 0.001$), suggesting that mineral retention dynamics are influenced by both the density and the surface-area-to-volume ratio of specific octopus' components. The highest mineral retention was observed in the head region processed using OSD (6.03 ± 0.04%), likely due to mineral concentration resulting from substantial organic mass loss under open drying conditions. Conversely, the MSD system was effective in preserving mineral integrity and provided greater physical protection against ambient contamination compared to open-air methods (Afzal et al. 2023).

Overall, the significant effect of anatomical parts on quality parameters underscores the critical role of morphology in determining final product quality. Thinner sections, such as the mantle, exhibited the best retention of quality, while thicker sections were more susceptible to degradation, highlighting the need for targeted drying protocols in cephalopod processing (Hajji et al. 2024).

CONCLUSION

The comparative performance of the MSD and OSD systems for octopus processing was systematically evaluated under tropical environmental conditions. Compared with OSD, MSD maintained a 20% higher average temperature (42.1 °C vs. 35.0 °C) and a 29% lower relative humidity (38.1% vs. 54.0%), resulting in a 74% increase in drying rate (0.47 vs. 0.27 $kg \cdot kg^{-1} \cdot h^{-1}$). Anatomical heterogeneity of octopus specimens significantly influenced drying kinetics. Thinner sections, such as the mantle, exhibited drying rates nearly double those of thicker regions, including the head and middle tentacles. Among the five thin-layer kinetic models evaluated, the Hasibuan and Daud model equation demonstrated the highest predictive accuracy ($R^2 = 0.9965$; RMSE = 0.0168; SSE = 0.0058), indicating its robustness for modelling complex biological matrices. Statistical analyses showed that the drying method significantly affected both protein retention and browning index, with the MSD providing superior outcomes due to effective shielding from direct ultraviolet radiation. Ash content displayed significant interaction effects between dryer type and anatomical region, while fat content was primarily determined by anatomical morphology ($P < 0.001$) rather than drying system ($P > 0.05$). The MSD is recommended as a highly energy-efficient engineering solution for premium octopus processing in coastal regions, supporting sustainable development goals (SDG) 7 and 9. For optimal industrial implementation, drying protocols should be tailored to anatomical thickness to ensure uniform quality and prevent over-drying of thinner tissues. Future research should focus on integrating advanced and consistent thermal energy sources to reduce kinetic variability across anatomical regions, especially under fluctuating environmental conditions.

Acknowledgement

The authors gratefully acknowledge the Department of Agricultural Technology, Faculty of Agriculture, University of Bengkulu, for providing the facilities and infrastructure essential for conducting this research.

REFERENCES

Acar C., Dincer I., Mujumdar A. (2022): A comprehensive review of recent advances in renewable-based drying technologies for a sustainable future. Drying Technology, 40: 1029–1050.

Afzal A., Iqbal T., Ikram K., Anjum M.N., Umair M., Azam M., Akram S., Hussain F., Ameen ul Zaman M., Ali A., Majeed F. (2023). Development of a hybrid mixed-mode solar dryer for product drying. Heliyon, 9: e14144.

Agyei T.A., Amponsah S., Kwadwo, Akowuah J.O., Addo A. (2025): Evaluating the performance of thin-layer drying models in predicting the drying behavior of catfish flesh under convective and microwave drying. Journal of Food Processing and Preservation, 2025: 1–14.

https://doi.org/10.17221/199/2025-RAE

Andharia J.K., Solanki J.B., Maiti S. (2023): Performance evaluation of a mixed-mode solar thermal dryer with black pebble-based sensible heat storage for drying marine products. Journal of Energy Storage, 57: 106186.

Bacha H., Ben Joseph A., Abdullah A.S., Sharshir S.W. (2025): Innovative experimental investigation of a solar dryer with an evacuated tube solar air heater and various thermal energy storage techniques. Case Studies in Thermal Engineering, 69: 106018.

Biswas R., Hossain M.A., Zzaman W. (2022): Thin layer modeling of drying kinetics, rehydration kinetics and color changes of osmotic pre-treated pineapple (*Ananas comosus*) slices during drying: Development of a mechanistic model for mass transfer. Innovative Food Science and Emerging Technologies, 80: 103094.

BSN (2006): SNI 01.2354.1-2006 Cara Uji Kimia – Bagian 1: Penentuan Kadar Abu pada Produk Perikanan. Jakarta, Badan Standarisasi Nasional.

BSN (2017): Cumi-cumi dan Sotong Kering. In: SNI 2719:2017. Jakarta, Badan Standarisasi Nasional

Budiyanto M.A., Nasrudin, Lubis M.H. (2020): Turbidity factor coefficient on the estimation of hourly solar radiation in Depok City, Indonesia. Energy Reports, 6: 761–766.

Chemkhi S. (2022): Design, manufacturing and test of a mixed-mode solar dryer for food products. In:13th Int. Renewable Energy Congr. (IREC). Hammamet, Dec 13–15, 2022: 1–5.

De Andrade R.C., Tiba C. (2016): Extreme global solar irradiance due to cloud enhancement in northeastern Brazil. Renewable Energy, 86: 1433–1441.

Deeto S., Thepa S., Monyakul V., Songprakorp R. (2018): The experimental new hybrid solar dryer and hot water storage system of thin layer coffee bean dehumidification. Renewable Energy, 115: 954–968.

Delfiya D.S.A., Murali S., Alfiya P.V., Samuel M.P. (2020): Drying characteristics of shrimp (*Metapenaeus dobsoni*) in electrical dryer. Pantnagar Journal of Research, 18: 280–284.

Duong Y.H.P., Vo N.T., Le P.T.K., Tran V.T. (2021): Three-dimensional simulation of solar greenhouse dryer. Chemical Engineering Transactions, 83: 211–216.

Ekka J.P., Palanisamy M. (2021): Performance assessments and techno and enviro-economic analyses on forced convection mixed mode solar dryer. Journal of Food Process Engineering, 44: 1–13.

European Union (2022): Musky Octopus. Mr. Goodfish. Available at https://www.mrgoodfish.com/en/seafood/musky-octopus-2/ (accessed Oct 19, 2025).

Fall A.D., Asiedu B. (2024): The artisanal octopus fishery in Mauritania: A lucrative fishery in decline. Marine Policy, 169: 106335.

Fatharani A., Maissy F., Yuwana Y., Anis U. (2025): Color instrument analysis of octopus drying using solar hybrid dryer. BIO Web of Conferences, 158: 1–9.

Fikry M., Benjakul S., Al-Ghamdi S., Tagrida M., Prodpran T. (2023): Evaluating kinetics of convection drying and microstructure characteristics of Asian seabass fish skin without and with ultrasound pretreatment. Foods, 12: 3024.

Ghanem T.H.M., Nsasrat L.S., Younis O.S., Metwally K.A., Salem A., Orban Z., Eid M.H., El-Mesery H.S., Eldin A.Z., Elmolakab K.M., Mahmoud S.F., Elwakeel A.E. (2025): Thin-layer modeling, drying parameters, and techno-enviro-economic analysis of a solar dried salted tilapia fish fillets. Scientific Reports, 15: 1–20.

Hajji W., Essid I., Bellagha S. (2024): Sun-dried and convective-dried *Octopus vulgaris* quality parameters and estimated shelf life during ambient temperature storage. Journal of Aquatic Food Product Technology, 33: 443–454.

Hernández-Urcera J., Soule S.E., Cabanellas-Reboredo M., González Á.F. (2025): Bivalve shell utilization by juvenile *Octopus vulgaris* in sandy substrates. Ecology and Evolution, 15: 1–5.

Hidrawati, Sahari S., Limi M.A., Surni, Rosna (2023): Study of mechanisms and income differences of octopus fishermen on the Bhanto Bhenta's local wisdom application in small islands areas. IOP Conference Series: Earth and Environmental Science, 1137: 012065.

Hii C.L., Chiang C.L., Putranto A. (2023): Modelling heat and mass transfer processes during drying: empirical, theoretical and reaction engineering approach. AIP Conference Proceedings, 2586: 060011.

Hu L., Kim D., Tyo J.S., Ritchie E.A. (2025): The impact of solar elevation angle on the net radiative effect of tropical cyclone clouds. Npj Climate and Atmospheric Science, 8: 67.

Hu Y., Zeng X., Jiang K., Luo Y., Quan Z., Li J., Ma Y., Guo X., Zhou D., Zhu B. (2024): Effect of non-enzymatic browning on oysters during hot air drying process: Color and chemical changes and insights into mechanisms. Food Chemistry, 454: 139758.

Indrabudi T., Triyanti R., Safitri W., Arief M.C. W. (2025): Socio-economic dynamics of octopus fisheries for the livelihood sustainability of small-scale fishers in East Java, Indonesia. BIO Web of Conferences, 156: 03013.

Inman R.H., Chu Y., Coimbra C.F.M. (2016): ScienceDirect Cloud enhancement of global horizontal irradiance in California and Hawaii. Solar Energy, 130: 128–138.

Inyang U.E., Oboh I.O., Etuk B.R. (2018): Kinetic models for drying techniques – Food materials. Advances in Chemical Engineering and Science, 8: 27–48.

Jonathan B.J., Egbe E.W. (2022): Thin layer drying kinetics of salt water crab (*Cardisoma guanhumi*). Saudi Journal of Engineering and Technology, 7: 165–171.

https://doi.org/10.17221/199/2025-RAE

Kuhe A., Ibrahim J.S., Tuleun L.T., Akanji S.A. (2019): Effect of air mass flow rate on the performance of a mixed-mode active solar crop dryer with a transpired air heater. International Journal of Ambient Energy, 43: 531–538.

Lakshmi D.V.N., Muthukumar P., Nayak P.K. (2021): Experimental investigations on active solar dryers integrated with thermal storage for drying of black pepper. Renewable Energy, 167: 728–739.

Mehta P., Bhatt N., Bassan G., Kabeel A.E. (2022): Performance improvement and advancement studies of mixed-mode solar thermal dryers: A review. Environmental Science and Pollution Research, 29: 62822–62838.

Nurba D., Mustaqimah, Fadhil R., Hadiyanto W. (2019). Design and performance test of solar vertical dryer for Salted fish. IOP Conference Series: Earth and Environmental Science, 365: 012046.

Obot N.I., Ajiboye A.A., Akanbi S.A., Chendo M.A.C. (2022): Croaker fish drying using artificially roughened surface collector solar system. Suranaree Journal of Science and Technology, 29: 020016.

Pariansyah A., Adharini R.I., Sari D.W.K., Hardianto E. (2025): Morphological, morphometric, and molecular identification of *Octopus cyanea* in the waters of Kaur District, Bengkulu Province, Indonesia. Biodiversitas, 26: 2640–2652.

Piacentini R.D., Salum G.M., Fraidenraich N., Tiba C. (2011): Extreme total solar irradiance due to cloud enhancement at sea level of the NE Atlantic coast of Brazil. Renewable Energy, 36: 409–412.

Sauer W.H., Gleadall I.G., Downey-Breedt N., Doubleday Z., Gillespie G., Haimovici M., Ibáñez C.M., Katugin O.N., Leporati S., Lipinski M., Markaida U., Ramos J.E., Rosa R., Villanueva R., Arguelles J., Briceno F.A., Carrasco S.A., Che L.J., Chen C.-S., Yamrungrueng A., et al. (2021): World octopus fisheries. Reviews in Fisheries Science and Aquaculture, 29: 279–429.

Schweidtmann A.M., Zhang D., von Stosch M. (2024): Review article. A review and perspective on hybrid modeling methodologies. Digital Chemical Engineering, 10: 100136.

Shen L., Chen F., Huang Q., Tan H., Ling Y., Qiu W., Zhou M., Liu D., Qiao Y., Wang L., Wang C., Wu W. (2024): Effect of light treatment on oxidation and flavour of dry-cured Wuchang fish. Food Chemistry, 22: 101464.

Sudarmadji S., Haryono B., Suhardi (1997): Prosedur Analisa untuk Bahan Makanan dan Pertanian. 4th Ed. Liberty.

Suherman S., Widuri H., Patricia S., Susanto E.E., Sutrisna R.J. (2020): Energy analysis of a hybrid solar dryer for drying coffee beans. International Journal of Renewable Energy Development, 9: 131–139.

Suherman S., Anggoro D.D., Sugiharto S., Asy-Syaqiq M.A. (2025): Investigation of a mixed-mode solar dryer assisted with an air recycling system and phase change material unit for coffee beans drying: An experimental study. Renewable Energy, 254: 123762.

Talumepa A.C.N., Suptijah P., Wullur S., Rumengan I.F.M. (2016): Kandungan Kimia dari Sisik Beberapa Jenis Ikan Laut. Jurnal LPPM Bidang Sains Dan Teknologi, 3: 27–33.

Vamvakas I., Salamalikis V., Kazantzidis A. (2020): Evaluation of enhancement events of global horizontal irradiance due to clouds at Patras, South-West Greece. Renewable Energy, 151: 764–771.

Vengsungnle P., Jongpluempiti J., Srichat A., Wiriyasart S., Naphon P. (2020): Thermal performance of the photovoltaic-ventilated mixed mode greenhouse solar dryer with automatic closed loop control for Ganoderma drying. Case Studies in Thermal Engineering, 21: 100659.

Wulfing S., Kadba A., Baker-Médard M., White E.R. (2024): Assessing the need for temporary fishing closures to support sustainability for a small-scale octopus fishery. Fisheries Research, 276: 107045.

Xue J., Ma J., Zhang X., Wang H., Chen S., Dai,Z. (2015): Nutritional analysis and evaluation of two marine octopus species. Journal of Chinese Institute of Food Science and Technology, 15: 203–211.

Xue J., Dai Z., Li K., Ma J., Wang H. (2020): Microflora changes of instant octopus products at different storage temperatures based on metagenomics. Chinese Institute of Food Science and Technology, 20: 226–233.

Yassen T.A., Al-Jethelah M.S.M., Dheyab H.S. (2021): Experimental study of innovative indirect solar dryers. International Journal of Heat and Technology, 39: 1313–1320.

Yuwana, Sidebang B., Silvia E. (2011): Temperature and relative humidity gains of "Teko Bersayap" model solar dryer (A research note). In: Int. Seminar of CRISU and CUPT "Exploring Research Potential" Session Energy, Education and Others. Palembang, January 2011: 221–227.

Zamuz S., Bohrer B.M., Shariati M.A., Rebezov M., Kumar M., Pateiro M., Lorenzo J.M. (2023): Assessing the quality of octopus: From sea to table. Food Frontiers, 4: 733–749.

Zhong S., Liu Y., Tian Z. (2020): Environment-friendly drying device based on distributed photovoltaic energy. IOP Conference Series: Earth and Environmental Science, 512: 012012.

Zuo H., Qiu J., Fan Y., Li F. (2024): Evaluating the cloud effect on solar irradiation by three-dimensional cloud information. Solar Energy, 272: 112489.

Received: November 11, 2025
Accepted: April 8, 2026
Published online: April 29, 2026